Stick Slip and Control in Low-Speed Motion

Brian Armstrong-Hélouvry

Abstract—**Dimensional and perturbation analysis are applied to the problem of stick slip encountered during the motion of machines. The friction model studied is motivated by current tribological results and is appropriate for lubricated metal contacts. The friction model incorporates Coulomb, viscous and Stribeck friction with frictional memory and rising static friction. Through dimensional analysis an exact model of the nonlinear system can be formed in five parameters rather than ten, greatly facilitating study and explicitly revealing the interaction of parameters. By converting the system of differential equations into a set of integrations, the perturbation technique makes approximate analysis possible where only numerical techniques had been available before. The analysis predicts the onset of stick slip as a function of plant and controller parameters; these results are compared with experimental data.**

I. Introduction

WHEN moving slowly, machines are likely to exhibit stick slip, a periodic cycle of alternating motion and arrest. Stick slip determines the lower performance bounds of a machine: the lowest sustainable speed and the shortest governable motion. In applications that place a premium on precise motion, an understanding of the dynamics of stick slip and its possible elimination take on great value.

A. Tribology and Controls

Systematic study of tribology, the science of rubbing interfaces, began early in this century and has made very considerable progress in the understanding of frictional phenomena, particularly of engineering materials. The controls literature concerned with friction is also considerable; highlights are discussed in Section I-B below. The controls-based investigation of friction, however, has not reached its full potential. This is due in part because the friction models used are sometimes simplistic and inadequate to represent the observed behavior of servo systems. Advantage has not been taken of the progress of tribology [22].

Space permits here only a brief outline of the tribological investigation of the frictional dynamics of lubricated metal-metal contacts. A more complete discussion of the results of tribology important for control may be found in [1], [2]. The evidence of the tribology literature justifies a friction model with Coulomb plus viscous friction—the components normally considered in the controls literature—and four additional components which shape the behavior of stick-slip motion in machines:

1) Stribeck Friction;
2) Rising Static Friction;
3) Frictional Memory;
4) Presliding Displacement.

The Stribeck curve is the shape of the friction versus velocity curve for lubricated systems, [1], [2], [11], [26], [30], and is illustrated in Fig. 1. The figure shows four regimes that will be observed in oil or grease lubricated contacts: No Sliding, where motion exists as the interface bonding sites deform elastically; Boundary Lubrication, where sliding occurs with solid-to-solid contact because the velocity is not adequate to entrain fluid lubricant into the junction; Partial Fluid Lubrication, where the velocity is adequate to entrain some fluid into the junction, but not enough to fully separate the surfaces; and Full Fluid Lubrication, where the surfaces are fully separated by a fluid film. The negative going portion of the curve arises from the contact riding up on a lubricant film in the regime of partial fluid lubrication: as the lubricant film grows thicker with increasing velocity, the friction decreases. This portion of the (friction–velocity) curve gives a substantial destabilizing effect. Tribology can not yet provide a physically motivated model of Stribeck friction. Of the empirical models that have been investigated, the model employed by Hess and Soom, [19], is used here because of its analytic tractability; the third term models the negative going regime of partial fluid lubrication:

$$F(t) = F_k \operatorname{sgn}(\dot{x}(t)) + F_v \dot{x}(t) + F_s(\gamma, t_2) \frac{1}{1 + \left(\frac{\dot{x}(t)}{\dot{x}_s}\right)^2} \operatorname{sgn}(\dot{x}(t)). \quad (1)$$

The notation is defined in Section I-C below; we note here that, whereas the Coulomb and viscous friction, F_k and F_v, are constant, the magnitude of the Stribeck friction, F_s, is a function of two parameters, reflecting the rising static friction.

The Model presented here has not considered time varying normal force, which will influence frictional memory and the Stribeck curve [23]. Varying normal force is considered briefly, but from a controls perspective, in [1] and more thoroughly in [23].

The static friction is the force required to initiate sliding; it is the breakaway force and the magnitude of the Stribeck friction evaluated with $\dot{x} = 0$. In lubricated machines the highest value of static friction, $F_{s,\infty}$ is not

Manuscript received March 27, 1992; revised December 8, 1992. Paper recommended by Past Associate Editor, J. W. Grizzle.

The author is with the Department of Electrical Engineering and Computer Science, University of Wisconsin-Milwaukee, Milwaukee, WI 53201.

IEEE Log Number 9211899.

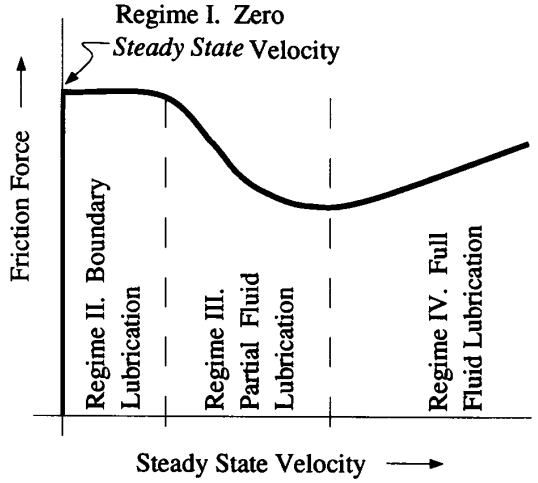

Fig. 1. The generalized Stribeck curve, showing friction as a function of velocity for low velocities.

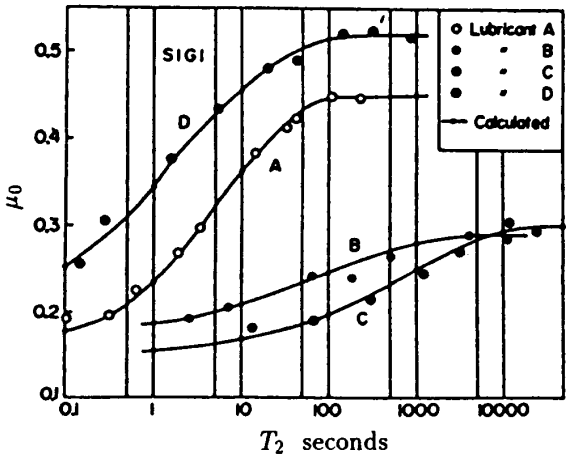

Fig. 2. Static friction (breakaway force) as a function of time at zero velocity (dwell time). μ_0 is the excess static friction over kinetic friction; T_2 is the dwell time, as in Fig. 7. Lubricants A, B, C and D are, respectively, viscous mineral oil, commercial slideway lubricant, castor oil and paraffin oil. (From Kato *et al.* [20], courtesy of the publisher.)

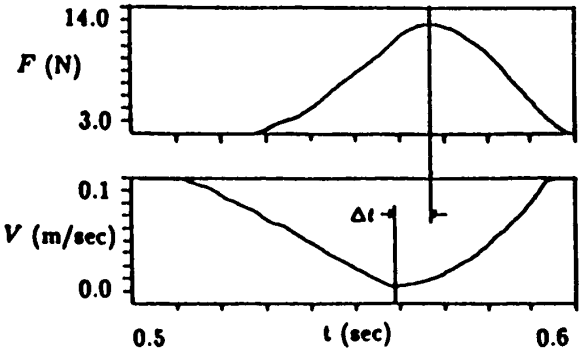

Fig. 3. Typical friction-speed time shift (frictional memory); contact load = 250 Newtons, lubricant viscosity = 0.322 Pa · s, motion frequency = 1 Hz. $F(N)$: friction, Newtons; V(m/s): velocity. (From Hess and Soom [19], courtesy of the publisher.)

reached at the instant that the machine arrives at zero velocity [2], [20], [25], [26]. Instead, in metal-to-metal contacts with standard lubricants, the static friction rises with time from a lower kinetic friction value to the higher, steady-state static friction level. Fig. 2 is from Kato *et al.* [20], where a good discussion of this phenomena may be found. Physically, rising static friction arises from the time required to expel the fluid lubricant film from the contact interface. For control, the implication is that if the residence time at zero velocity is sufficiently short, the stick slip inducing, excess static friction will be reduced, and stick slip will be extinguished [13], [26]. As we will see, this process dominates the extinction of stick slip as velocity rises. Rising static friction is modeled [20]:

$$F_{s,b_n} = F_{s,a_{n-1}} + (F_{s,\infty} - F_{s,a_{n-1}})\frac{t_2}{t_2 + \gamma} \qquad (2)$$

where F_{s,b_n} is the magnitude of Stribeck friction at the beginning of the nth slip; F_{s,b_n} is also the static friction or breakaway force of the nth stick-slip cycle. $F_{s,a_{n-1}}$ is the Stribeck friction magnitude at the end of the $(n-1)^{st}$ slip; t_2, the dwell time, is the period spent in the stuck condition; and γ, a friction parameter, is the rising static friction rate. A subscript 'b' indicates a quantity evaluated at breakaway, and 'a' at arrest. Definitions of sub and superscripts and other symbols are provided in Section I-C below.

In systems ranging from rock mechanics, [27], through lubricated machines, [2], [6], [7], [19], [26], to numerical analysis of transient partial-elasto-hydrodynamic lubrication, [36], a time lag, or phase shift, has been observed between a change in the sliding velocity and the corresponding change in friction. When velocity changes, the friction does not change instantly, but adjusts to its new steady state value only after some time. Fig. 3 is taken from the experimental data of Hess and Soom [19] and shows clearly the frictional memory. Physically, frictional memory is the result of state in the interface (lubricant film thickness is almost certainly one state variable [23]) which must adjust to the new sliding condition before the friction force will attain its new value. Hess and Soom, [19], present experimental support for a simple lag model. The experiments of Hess and Soom, which did not incorporate breakaway from zero velocity, have recently been extended by Polycarpou and Soom, [24], to include detailed friction measurements of the transition from stiction to sliding. Dupont, [14], and Rice and Ruina, [27], argue for a state variable model. Here the simple lag model will be used:

$$F_t(t) = F_{\dot{x}}(\dot{x}(t - \tau_L)). \qquad (3)$$

Where F_t is friction as a function of time, and $F_{\dot{x}}$ is friction as a function of velocity, (1).

Presliding displacement is a consequence of elastic deformation of the surface asperities where contact and sliding occur and significantly influences friction forces during velocity reversal [2], [5], [12], [18]. It is the compliance of presliding displacement that softens the hard nonlinearity of friction at zero velocity, and may make feasible some of the high gain controllers that are found in applications [1]. In this paper, uniform sliding without velocity reversal is considered and so the state of elastic deformation is constant. Presliding displacement will not be considered further.

The absence of these three frictional phenomena—Stribeck friction, rising static friction and frictional memory—from the models investigated in the controls literature has limited the ability of the control theoretic investigations to describe the physical behavior of systems. For example, a considerable literature exists applying describing function analysis to a system with Coulomb plus viscous plus, most often, static friction (the C + V + S model), and investigating the resulting amplitude-dependent stability (a test for limit cycling or stick-slip motion) e.g., [10], [17], [29], [31], [32]. A difficulty arises because these analyses do not predict stick-slip motion for a second order system in the absence of integral control [10]; while, in fact mechanisms governed by PD controllers are observed to stick slip. A friction model incorporating nonlinear, low-velocity friction is required to account for the observed behavior.

By applying dimensional analysis, it has been shown that in a second-order system with C + V + S friction, increasing stiffness should not extinguish stick slip over a broad range of system conditions [4]. Experience, however, shows that increasing stiffness often extinguishes stick slip (see Fig. 4 below; and, indeed, stiffening a component is a standard technique in mechanical design for eliminating chatter.) The interaction of stiffness and stick slip is a consequence of frictional phenomena not considered in the C + V + S model.

And the extinction of stick slip with increasing velocity, while qualitatively anticipated by investigation of the C + V + S model, is not quantitatively described correctly. As early as the 1950's, it was known within the tribology community that static friction rises as a junction spends more time at rest, and that this rising static friction has a pronounced influence on the continued occurrence of the stick-slip limit cycle. Derjaguin *et al.*, [13], investigate the influence of this phenomenon. In [25], Rabinowicz shows that rising static friction plays an important role in explaining the force cycle observed during stick slip. This can be seen in Fig. 4, where increasing stiffness corresponds to decreasing stick-slip amplitude. This relation arises because the stiffer system spends less time at zero velocity and thus has less static friction.

The combined impact of these influences is that the literature concerned with servo control of machines with friction does not present a predictive capability. The works of Tou and Schultheiss, [31], Shen, [29], Walrath, [35], Canudas and Seront, [10], and others *qualitatively* describe the observed limit-cycle behavior; but cannot quantitatively predict the presence, absence or character of this behavior in real mechanisms based on parameters of the friction model and control system.

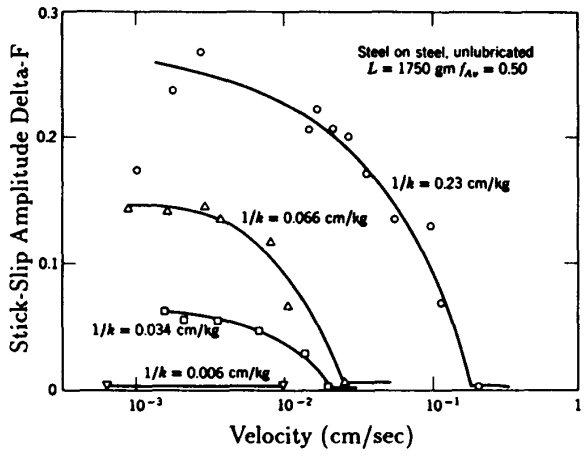

Fig. 4. Stick-slip amplitude as a function of velocity, for several spring stiffness. (From Rabinowicz [25], courtesy of the publisher.)

B. Prior Work within Controls

An overview of the controls literature concerned with friction and stick slip can be found in [1], [2], [16]. Several papers are mentioned here because they include parts of the friction model described. Tustin, [33], employs an exponential friction-velocity relation that is a form of the Stribeck curve. He uses a graphic method of analysis to determine conditions for stick slip. Significantly, his analysis shows that stick slip can occur in the absence of an integral control term. Recently a number of investigators have employed friction models incorporating Stribeck friction [2]–[5], [10], [15], [16]. These investigations have shown that the Stribeck friction influences the presence of stick slip and the stability of adaptive friction compensation.

Derjaguin *et al.*, [13], published in the tribology literature, but their paper is concerned with the dynamics of a mass-spring-slider system that mirrors a servo mechanism with PD control. By employing a C + V + S model, without Stribeck friction or frictional memory but considering rising static friction, they are able to form exact integrals of the system equations of motion. In this way they find velocity dependence in the presence of stick slip that is similar to that observed experimentally. The terms derived in their dimensional analysis are comparable to the terms derived here.

Dupont, [14], studies the influence of a state variable friction model on the stability of feedback control. The state variable friction model has its roots in rock mechanics [27] and is an alternative to the time lag employed here. As here, though by a very different method of analysis, Dupont finds that stick slip can be eliminated by sufficiently stiff *position* control.

The system to be analyzed consists of a sliding mass governed by a proportional-derivative (PD) controller. The sliding contact friction combines Stribeck friction, frictional memory and rising static friction. In analysis, the dynamics of ideal PD control are interchangeable with the those of a mass-spring system with damping. The combined dynamic is expressed:

$$M\ddot{x} = -k_p x - k_v \dot{x} - F_k \operatorname{sgn}(\dot{x}) - F_v \dot{x} - F_{s,b_n}(\gamma, t_2)\Psi(\dot{x}/\dot{x}_s, \tau_L)\operatorname{sgn}(\dot{x}); \quad (4)$$

$$\Psi(\dot{x}/\dot{x}_s, \tau_L) = \begin{cases} \dfrac{1}{1 + \left(\dfrac{\dot{x}(t-\tau_L)}{\dot{x}_s}\right)^2}, & t > \tau_L \\ 1, & t \le \tau_L \end{cases}; \quad (5)$$

$$F_{s,b_n} = F_{s,a_{n-1}} + (F_{s,\infty} - F_{s,a_{n-1}})\frac{t_2}{t_2 + \gamma}. \quad (6)$$

The notation used is defined below. The friction model is made up of F_k and F_v, the customary Coulomb and viscous friction terms, and $F_{s,b_n}(\cdot)\Psi(\cdot)$, which models the Stribeck friction. The Stribeck friction model is divided into two components: the magnitude on the n^{th} stick-slip cycle, $F_{s,b_n}(\cdot)$, which has dimensions of force, depends upon the dwell time and is used to model rising static friction; and a velocity dependent term, $\Psi(\cdot)$, which is dimensionless, ranges from zero to one and incorporates the Stribeck friction curve and frictional memory. $F_{s,a_{n-1}}$ is the magnitude of Stribeck friction at the end of the $(n-1)^{st}$ stick-slip cycle; the details of the Stribeck friction magnitude model are presented more fully in Section IV below. The case statement in the definition of $\Psi(\cdot)$ is used to reflect the fact that $\Psi(\cdot) = 1$ prior to sliding. The physical dimensions of linear sliding are used here: with appropriate changes of dimension, rotational motion may be considered by the same analysis.

C. Nomenclature

[units given for translational motions]

M = mass, [kg]
k_p = stiffness, [Newtons/m]
k_v = deriv. feedback or damping, [Newtons/m s^{-1}]
F = total friction force, [Newtons]
F_k = kinetic friction, [Newtons]
F_k^* = dimensionless kinetic friction; $F_k^* = (F_k/M/\alpha\beta^2)$
F_v = viscous friction, [Newtons/m s^{-1}]
$F_s(\cdot)$ = instantaneous magnitude of the Stribeck friction, [Newtons]
$F_{s,\infty}$ = magnitude of the Stribeck friction after long time in contact, [Newtons]
F_{s,b_n} = magnitude of the Stribeck friction at time t_b on the nth stick-slip cycle, [Newtons]
$F_{s,a_{n-1}}$ = magnitude of the Stribeck friction at time t_a $F_{s,a}$ on the $(n-1)^{th}$ stick-slip cycle, [Newtons]
$F_{s,b_{ss}}$ = steady state magnitude of the Stribeck friction, [Newtons]
$F^*_{s,\infty}$ = dimensionless $F_{s,\infty}$, [·]
F^*_{s,b_n} = the dimensionless Stribeck friction at break-away of the n^{th} stick-slip cycle, [·]
$F^*_{s,b_{ss}}$ = dimensionless $F_{s,b_{ss}}$, [·]
$\Psi(\cdot)$ = velocity and frictional memory dependence in Stribeck friction, [·]
$\Psi^*(\cdot) = \Psi(\cdot)$ in dimensionless coordinates, [·]
$k'_v = k_v + F_v$; merged damping and viscous friction
$\omega = \sqrt{k_p/M}$; the natural frequency, [s^{-1}]
$\rho = k'_v/2\omega$; the damping factor, [·]
$x, \dot{x}, \ddot{x}$ = position, velocity and acceleration in physical coordinates, [m], etc.
$\xi, \dot{\xi}, \ddot{\xi}$ = position, velocity and acceleration in dimensionless coordinates, [·]
ξ_b = dimensionless position at the moment of break-away
ξ_a = dimensionless position at the moment of arrival in static friction
$\dot{x}_d$ = desired sliding velocity, [m s^{-1}]
$\dot{\xi}_d$ = dimensionless desired velocity; $\dot{\xi}_d = \dot{x}_d/\dot{x}_s$, [·]
$\dot{x}_s$ = characteristic velocity of the Stribeck friction, [m s^{-1}]
$\alpha = \dot{x}_s/\omega$; scaling factor for length, [m]
$\beta = \omega$, scaling factor for time, [s^{-1}]
t = time, [s]
t_1 = duration of the slip portion of the stick-slip cycle, [s]
t_2 = duration of the stick portion of the stick-slip cycle, dwell time, [s]
γ = characteristic time of the static friction rise, [s]
τ_L = magnitude of the time lag in sliding friction, [s]
$t^*, t_2^* = t, t_2$, in dimensionless coordinates, [·]
$\gamma^*, \tau_L^* = \gamma, \tau_L$, in dimensionless coordinates, [·]
$\vec{r}$ = radius vector of a trajectory in the phase plane, Fig. 7
E_k^* = dimensionless kinetic energy, [·]
$\Delta_{E^*_{\text{slip}}}$ = change in dimensionless kinetic energy during slip, [·]
$\Delta_{E^*_\rho}$ = energy dissipated during a slip cycle by damping, [·]
$\Delta_{E^*_w}$ = energy contributed to a slip cycle by spring windup, due to static friction, [·]
$\Delta_{E^*_{Fs}}$ = perturbation to the slip energy due to Stribeck friction, [·]
$\Delta'_{E^*_{Fs}}$ = velocity and frictional memory dependent portion of $\Delta_{E^*_{Fs}}$, [·]
t_b = time at the moment of break-away, [s]
t_a = time at the moment of arrival in static friction, [s]

$t_b^*, t_a^* = t_b, t_a$ in dimensionless coordinates, [·]
h = static friction reduction factor, [·]
sgn(·) the signum function

Subscripts: b marks a variable given at the moment of break-away, the commencement of slip in the stick-slip cycle
a marks a variable given at the moment of arrival in static friction, the end of slip in the stick-slip cycle
Superscripts: * indicates a dimensionless quantity

II. Dimensional Analysis

The system under study is modeled as a nonlinear differential equation in the system state, (4), coupled to a nonlinear difference equation in the magnitude of static friction, (6). The combined system is one of 9 parameters, M, k_p, k_v, $F_{s,\infty}$, γ, $\dot{x}_s$, τ_L, F_k, and F_v. We shall consider the situation in which the desired motion is steady, i.e., $\dot{x}_d$ is a constant, creating a tenth parameter. The object of this paper is to determine the range of these parameters over which such a system will exhibit stick slip.

Dimensional analysis will provide a reduction in the number of independent parameters from 10 to 5, yielding a simpler model and greatly facilitating the perturbation analysis to follow. The first transformation is a shift of the position coordinate to place the equilibrium point at the origin. Physically, this shift corresponds to finding the point at which the proportional term balances the Coulomb Friction and the viscous and Stribeck friction due to steady motion. The shift eliminates the parameter F_k from the dynamic equation. Folding the viscous friction parameter into the derivative feedback, one may write $k_v' = k_v + F_v$. Defining:

$$x' = x - x_d + \frac{\left\{F_k + k_v'\dot{x}_d + F_s(\gamma, t_2)\Psi\left(\frac{\dot{x}_d}{\dot{x}_s}, 0\right)\right\}}{k_p};$$

then

$$\dot{x}' = \dot{x} - \dot{x}_d,$$

$$\ddot{x}' = \ddot{x}. \tag{7}$$

(Note: $\ddot{x}' = \ddot{x}$ because $\ddot{x}_d = 0$, only steady desired motion is considered.)

With this shift of the position coordinate, (4) becomes:

$$M\ddot{x}' = -k_p x' - k_v'\dot{x}' - F_s(\gamma, t_2)\left[\Psi\left(\frac{(\dot{x}' + \dot{x}_d)}{\dot{x}_s}, \tau_L\right) - \Psi\left(\frac{\dot{x}_d}{\dot{x}_s}, 0\right)\right]. \tag{8}$$

The $\operatorname{sgn}(\dot{x})$ functions are eliminated: when the commanded motion, $\dot{x}_d$, is steady motion in one direction, the velocity will not reverse under quite general circumstances [13]. Equation (8), coupled with (6), has 8 independent parameters, $\dot{x}_d$ included, in 3 physical dimensions: mass, length and time. The Buckingham Pi theorem, [8], indicates that the system may be described by (8–3) dimensionless groups. Scaling the position coordinate by a factor α, and the time coordinate by a factor $1/\beta$ gives dimensionless position and time, ξ and t^*:

$$\alpha\xi \equiv x' \quad \text{and} \quad t^* \equiv \beta t. \tag{9}$$

Forming the derivatives of ξ w.r.t. the new time coordinate, we find that

$$\frac{dx'}{dt} = \alpha\beta\frac{d\xi}{dt^*} \quad \text{and} \quad \frac{d^2x'}{dt^2} = \alpha\beta^2\frac{d^2\xi}{dt^{*2}}. \tag{10}$$

Substituting ξ for x' and its derivatives in (8) gives:

$$M\alpha\beta^2\ddot{\xi} = -k_p\alpha\xi - k_v'\alpha\beta\dot{\xi} - F_s(\gamma^*, t_2^*) \cdot\left[\Psi\left(\frac{\alpha\beta\left(\dot{\xi} + \dot{\xi}_d\right)}{\dot{x}_s}, \tau_L^*\right) - \Psi\left(\frac{\alpha\beta\dot{\xi}_d}{\dot{x}_s}, 0\right)\right], \tag{11}$$

where $\dot{\xi}_d$ is the magnitude of the desired velocity in dimensionless coordinates;

$$\alpha\beta\dot{\xi}_d = \dot{x}_d, \quad \gamma^* = \beta\gamma, \quad \text{and} \quad \tau_L^* = \beta\tau_L;$$

(Note: $\dot{\xi} = 0$ is the desired dimensionless velocity, not $\dot{\xi} = \dot{\xi}_d$).

Dividing through by the mass yields a system with scaled force constants. Writing (11) in terms of ω and ρ, the customary second order system parameters, and dividing through by $\alpha\beta^2$ gives:

$$\ddot{\xi} = -\frac{\omega^2}{\beta^2}\xi - 2\rho\frac{\omega}{\beta}\dot{\xi} - \frac{F_s(\gamma^*, t_2^*)/M}{\alpha\beta^2} \cdot\left[\Psi\left(\frac{\alpha\beta\left(\dot{\xi} + \dot{\xi}_d\right)}{\dot{x}_s}, \tau_L^*\right) - \Psi\left(\frac{\alpha\beta\dot{\xi}_d}{\dot{x}_s}, 0\right)\right]. \tag{12}$$

By choosing the time scale, β, to eliminate ω and the length scale, α, to eliminate $\dot{x}_s$, the dimensionless dynamic model is formed:

$$\beta = \omega = \sqrt{k_p/M} \quad \text{and} \quad \alpha = \frac{\dot{x}_s}{\beta} = \frac{\dot{x}_s}{\omega}. \tag{13}$$

Giving the dynamic equation

$$\ddot{\xi} = -\xi - 2\rho\dot{\xi} - F_{s,b_n}^*(\gamma^*, t_2^*)\Psi^*\left(\dot{\xi}, \tau_L^*\right), \tag{14}$$

where $\rho = (k_v^*/M)/2\omega$ and

$$F^*_{s,b_n} = F^*_{s,a_{n-1}} + (F^*_{s,\infty} - F^*_{s,a_{n-1}})\frac{t_2^*}{t_2^* + \gamma^*} \tag{15}$$

$$\Psi^*(\dot{\xi}, \tau_L^*) = \begin{cases} \dfrac{1}{1 + \left(\dot{\xi}(t^* - \tau_L^*) + \dot{\xi}_d\right)^2} - \dfrac{1}{1 + \left(\dot{\xi}_d\right)^2} = \dfrac{-\dot{\xi}(t^* - \tau_L^*)\left(\dot{\xi}(t^* - \tau_L^*) + 2\dot{\xi}_d\right)}{\left(1 + \left(\dot{\xi}(t^* - \tau_L^*) + \dot{\xi}_d\right)^2\right)\left(1 + \left(\dot{\xi}_d\right)^2\right)}, & t^* > \tau_L^* \\ 1 - \dfrac{1}{1 + \left(\dot{\xi}_d\right)^2} = \dfrac{\left(\dot{\xi}_d\right)^2}{1 + \left(\dot{\xi}_d\right)^2}, & t^* \le \tau_L^* \end{cases} \tag{16}$$

and where $F_s(\gamma^*, t_2^*) = ((F_s(\gamma^*, t_2^*)/M)/(\alpha\beta^2) = ((F_s(\gamma^*, t_2^*)/M)/(\omega\dot{x}_s))$; $\tau_L^* = \tau_L\omega$.

The dimensionless model is given by (13)–(16), a nonlinear differential and difference system in the five parameters ρ, $F^*_{s,\infty}$, $\dot{\xi}_d$, τ_L^*, and γ^*. By setting $\beta = \omega$ time measurements are scaled to units of the natural frequency of the system. Thus as stiffness increases, perhaps due to an increase in control gain, τ_L^* and γ^* increase as well. By scaling lengths according to $\alpha = \dot{x}_s/\omega$, the characteristic velocity of the Stribeck friction becomes the unit velocity. Thus, systems are scaled so that the range of motion velocity influenced by Stribeck friction, a range which will vary between systems, will correspond to dimensionless velocities of a fixed range. Roughly speaking, the dimensionless velocities influenced by Stribeck friction lie in the range from zero to ten. The dimensionless system has unit stiffness, that is k_p^*, if it were considered, would always equal one. As physical stiffness changes both α and β change, and thus the scaling is changed for all of the parameters and state variables.

In the dimensionless coordinates energy is proportional to radius on the phase plane, $(\xi^2 + \dot{\xi}^2)$ (when discussing the energy of a system under feedback control, the proportional term is treated as a virtual spring).

Writing in shifted physical coordinates, the system energy is given by:

$$E = \frac{1}{2}k_p x'^2 + \frac{1}{2}M\dot{x}'^2 = \frac{1}{2}k_p\frac{\dot{x}_s^2}{\omega^2}\xi^2 + \frac{1}{2}M\dot{x}_s^2\,\dot{\xi}^2 = \frac{1}{2}M\dot{x}_s^2\left(\xi^2 + \dot{\xi}^2\right). \tag{17}$$

Energy in dimensionless coordinates is given by:

$$E^* = \frac{1}{2}\left(\xi^2 + \dot{\xi}^2\right). \tag{18}$$

The derivation of the dimensionless model does not depend on the structure of the friction model, except to the extent that the Stribeck friction is modeled as a function of $(\dot{x}/\dot{x}_s)$. Thus, as tribological understanding improves and new friction models are presented, the dimensional analysis can be adapted.

III. Perturbation Analysis

Equations (13)–(16) present the coupled differential and difference equations governing the low velocity motion of a servo controlled mechanism. No analytic solution of equation (14) is available. And, while simulation is a useful tool in specific instances, the model has five independent parameters, creating a space of systems too large to fully explore numerically. To determine the parameter combinations that signal the onset of stick-slip motion, a perturbation technique will be used.

The unperturbed system is taken to be the full system less the viscous and Stribeck friction terms and less static friction, which is modeled by F_{s,b_n}, the Stribeck friction at the beginning of the n^{th} stick-slip cycle. The trajectory of the unperturbed system is simply a circle on the phase plan, centered at the origin and of radius $\dot{\xi}_d$. The trajectory of a sample stick-slip cycle and the corresponding unperturbed trajectory are shown in Fig. 5. The sample trajectory was generated by numerically integrating (14) with the parameters $F^*_{s,\infty} = 11.4$; $\gamma^* = 2.0$; $\tau_L^* = 1.0$; $\dot{\xi}_d = 0.75$ and $\rho = 0.3$. (A full investigation of friction in a Unimate PUMA robot arm is presented in [5], [2]; these are reasonable data for the base joint of that mechanism.) The circle is the corresponding unperturbed trajectory. This sample was selected to lie near the boundary at which stick slip is eliminated.

Using the unperturbed trajectory the influence of damping and the friction forces can be calculated as perturbations. The problem is converted in this way from one of analyzing a differential equation, (14), into one of integrating a set of equations along a fixed path. Stick slip can be detected as a condition on the sum of the energy contributions of the perturbation terms. The usefulness of this analysis rests on the fact that the perturbation terms, viscous and Stribeck friction, depend only on velocity, and, for a broad range of system parameters, the velocity profile of the unperturbed system is a good approximation to the velocity profile of the full system. This is particularly true near the stability boundary, where the perturbations sum to zero. Fig. 6 is a plot of the velocity profile of the sample trajectory of Fig. 5 and the corresponding unperturbed trajectory. The sample trajectory has been adjusted in time to show the correspondence of the sample and unperturbed trajectories. The two trajectories are substantially separated on the phase plane because their positions diverge as the integral of differences in velocity, but the velocities themselves are quite similar. Note that

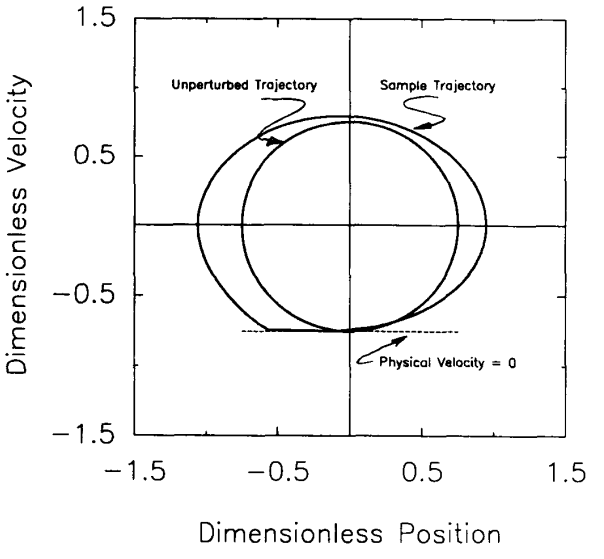

Fig. 5. Phase plane trajectories of a sample stick-slip cycle and the corresponding unperturbed trajectory.

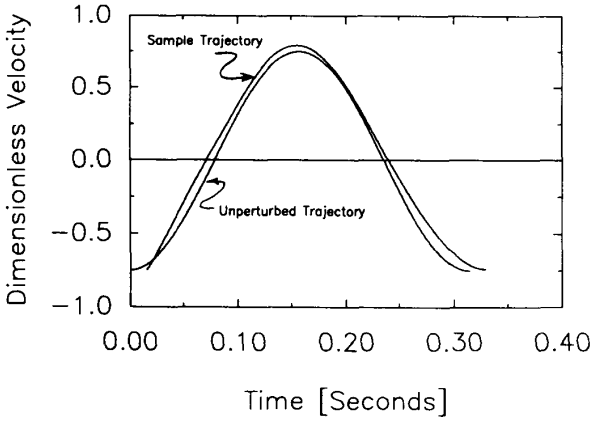

Fig. 6. Velocity profiles of the slip phases of the sample and unperturbed trajectories of figure 5. A time offset has been added to the sample trajectory.

the perturbation term does not depend upon position, but only upon velocity. Experimental evidence also supports this choice of unperturbed trajectory. In data of [3], [4], it is observed that over a factor of 20 range in stiffness and 30 range in velocity the slip distance of a stick-slip cycle is closely approximated by $x_{\text{slip}} = 2\pi\omega\dot{x}_d$; that is, the period of the unperturbed system times the desired velocity.

Fig. 7 illustrates the definitions of terms used in this analysis. The axes of the plane are dimensionless position, ξ, and velocity, $\dot{\xi}$. Terms referring to breakaway are subscripted 'b', thus $F_{s,b}$ is the level of Stribeck friction at breakaway, and F_{s,b_n} is the level of friction at breakaway of the n^{th} stick-slip cycle. The position at the moment of breakaway is ξ_b; and r_b is the radius of the trajectory at breakaway. The energy of the system at breakaway is

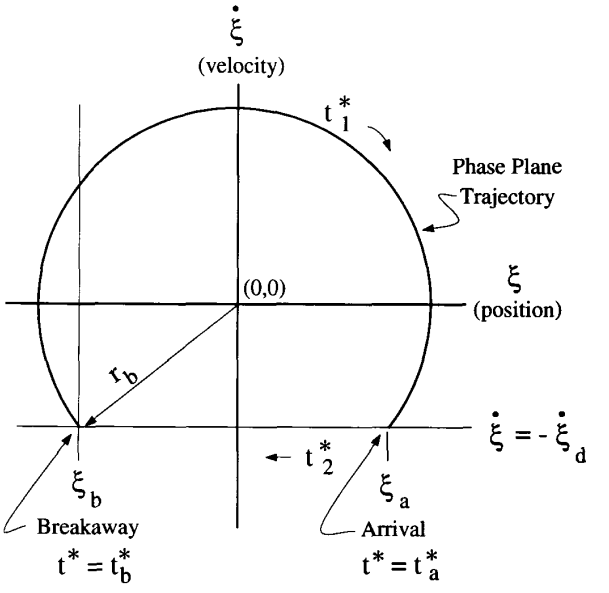

Fig. 7. Illustration of symbols used in the analysis.

given by $E^* = (1/2)r_b^2$. Because $\dot{\xi} = 0$ describes the system moving at the desired velocity, $\dot{\xi} = -\dot{\xi}_d$ corresponds to the system with a physical velocity of zero, i.e., in the stuck condition. The time t_1^* is the (dimensionless) time spent during the slip portion of the cycle, and t_2^* is the time of the stick portion of the cycle. The time of breakaway is designated t_b and the time of arrival into the stuck condition as t_a; thus, the time of sliding is the interval from t_b to t_a.

We are concerned with the kinetic energy at the end of an orbit on the phase plane. The dimensionless energy at breakaway is $E_k^* = 1/2r_b^2 = 1/2(\dot{\xi}_d^2 + \xi_b^2)$. To interrupt the limit-cycle of stick slip, the velocity after an orbit on the phase plane must not reach $\dot{\xi} = -\dot{\xi}_d$ ($\dot{x} = 0$ in physical coordinates). This gives rise to the condition that:

$$\Delta_{E^*_{\text{slip}}} < -\Delta_{E^*_w} \tag{19}$$

where $\Delta_{E^*_{\text{slip}}}$ is the change in dimensionless kinetic energy during the slip cycle; and $\Delta_{E^*_w} = 1/2\xi_b^2$ is the degree by which $1/2r_b^2$ exceeds $1/2\dot{\xi}_d^2$. The position of breakaway, ξ_b, is the point at which the spring force exceeds the friction. In dimensionless coordinates, considering the shift of origin, it is given by:

$$\xi_b = F^*_{s,b_n}\frac{\dot{\xi}_d^2}{1+\dot{\xi}_d^2}. \tag{20}$$

Equation (19) is a statement of the condition that more energy must be dissipated during the slip cycle than is provided to the system by spring windup (position feedback) at breakaway. Only systems which exhibit steady motion or bounded frictional instability are considered here. Neglected are systems with divergent modes of instability, such as k_p negative.

The change during an orbit of the dimensionless kinetic energy may be written:

$$\Delta_{E^*_{\text{slip}}} = \int_{t_b^*}^{t_a^*} \left(-2\rho\dot{\xi} - F^*_{s,b_n}\Psi^*\left(\dot{\xi}, \tau_L^*\right)\right)\dot{\xi}\, dt^*;$$

$$= -\int_{t_b^*}^{t_a^*} 2\,\rho\,\dot{\xi}\,\dot{\xi}\, dt^* - \int_{t_b^*}^{t_a^*} F^*_{s,b_n}(\gamma^*, t_2^*)\Psi^*\left(\dot{\xi}, \tau_L^*\right)\dot{\xi}\, dt^*. \tag{21}$$

Or written

$$\Delta_{E^*_{\text{slip}}} = \Delta_{E^*_\rho} + \Delta_{E^*_{Fs}} \tag{22}$$

where $\Delta_{E^*_\rho}$ and $\Delta_{E^*_{Fs}}$ are symbols for the respective integrals: $\Delta_{E^*_\rho}$ is the energy dissipated by the damping term; and $\Delta_{E^*_{Fs}}$ is the energy contributed or dissipated by the Stribeck friction. Exact evaluation of (21) would require knowledge of the state along the trajectory, which is to say the solution of (14). As a calculable approximation, (21) can be integrated along the path of the unperturbed trajectory.

The specifications of the unperturbed trajectory are:

$$\xi(t^*) = -\dot{\xi}_d \sin(t^*); \quad \dot{\xi}(t^*) = -\dot{\xi}_d \cos(t^*);$$
$$0 \le t^* \le 2\pi; \tag{23}$$

where $\dot{\xi}_d$ is the radius of the circle on the phase plane.

Using the trajectory of (23) in the first integral of (22) gives the energy dissipated by damping:

$$\Delta_{E^*_\rho} = -\int_0^{2\pi} 2\,\rho\,\dot{\xi}\,\dot{\xi}\, dt^* = -2\,\pi\,\rho\,\dot{\xi}_d^2. \tag{24}$$

The second integral in (22) is the change in system energy due to nonlinear friction. Integrating along the unperturbed trajectory gives:

$$\Delta_{E^*_{Fs}} = -F^*_{s,b_n}\left(\int_0^{\tau_L^*} \dot{\xi}(t^*)\, dt \right.$$
$$+ \int_{\tau_L^*}^{2\pi} \frac{\dot{\xi}(t^*)\, dt^*}{\left(\dot{\xi}(t^* - \tau_L^*) + \dot{\xi}_d\right)^2 + 1}$$
$$\left. + \int_0^{2\pi}\left(-\frac{1}{1+\dot{\xi}_d^2}\right)\dot{\xi}(t^*)\, dt^*\right)$$
$$= -F^*_{s,b_n}\dot{\xi}_d\left((-\sin(\tau_L^*))\right.$$
$$\left. + \int_{\tau_L^*}^{2\pi} \frac{(-\cos(t^*))\, dt^*}{\dot{\xi}_d^2(1 - \cos(t^* - \tau_L^*))^2 + 1} + 0\right). \tag{25}$$

Separating the integral from the multiplicative factors yields:

$$\Delta_{E^*_{Fs}} = F^*_{s,b_n}\dot{\xi}_d\Delta'_{E^*_{Fs}} \tag{26}$$

where

$$\Delta'_{E^*_{Fs}} = \sin(\tau_L^*) + \int_{\tau_L^*}^{2\pi} \frac{\cos(t^*)}{\dot{\xi}_d^2(1 - \cos(t^* - \tau_L^*))^2 + 1}\, dt^*. \tag{27}$$

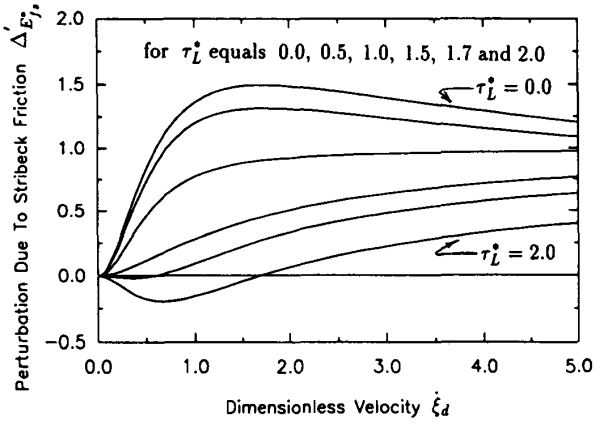

Fig. 8. The integral of (27) evaluated numerically as a function of $\dot{\xi}_d$ and τ_L^*.

The integral of (27) cannot be evaluated analytically, but can be evaluated numerically as a function of its two independent parameters, $\dot{\xi}_d$ and τ_L^*. The result of this numerical evaluation is shown in Fig. 8, where radial perturbation is plotted as a function of $\dot{\xi}_d$ and τ_L^*. Fig. 8 shows that as the frictional memory grows larger the destabilizing influence of the nonlinear friction is reduced.

Combining the terms of (22) and the condition for eliminating stick slip, $(\Delta_{E^*_{\text{slip}}})$ gives the condition for steady motion:

$$-2\,\pi\,\rho\,\dot{\xi}_d^2 + F^*_{s,b_n}\dot{\xi}_d\,\Delta'_{E^*_{Fs}} < -\frac{1}{2}\left(F^*_{s,b_n}\frac{\dot{\xi}_d^2}{1+\dot{\xi}_d^2}\right)^2. \tag{28}$$

Equation (28) provides the condition, in dimensionless coordinates, for eliminating stick slip. The role of stiffness in eliminating stick slip can be investigated by rewriting (28) in physical coordinates, separating out the dependency on stiffness, and combining all of the other terms into lumped parameters; giving:

$$\frac{1}{\sqrt{k_p}}(a - b) < -\frac{1}{k_p}c \tag{29}$$

where

$$a = \frac{F_{s,b_n}/\sqrt{M}}{\dot{x}_s}\frac{\dot{x}_d}{\dot{x}_s}\Delta'_{E^*_{Fs}}$$

$$b = \pi k'_v\sqrt{M}\,(\dot{x}_d/\dot{x}_s)^2$$

$$c = \frac{1}{2}\left(\frac{F_{s,b_n}/\sqrt{M}}{\dot{x}_s}\frac{\dot{x}_d^2}{\dot{x}_s^2 + \dot{x}_d^2}\right)^2.$$

When $(a - b) < 0$ (when damping is a greater influence than Stribeck friction) there exists a value of stiffness above which (29) is verified and stick slip will be extinguished. In the absence of frictional memory, $\Delta'_{E^*_{Fs}}$, and

therefore a, would be strictly positive and there would exist systems, particularly lightly damped systems, for which $(a - b) > 0$ and (29) is not verified for any value of stiffness. In the presence of frictional memory, however, $\Delta'_{E^*_{F_s}}$, and therefore a, decreases and finally becomes negative with increasing stiffness, as indicated by Fig. 8, and $(a - b) < 0$ is assured. Frictional memory explains the observed fact that across a broad range of mechanical systems, stick slip can be eliminated by increasing stiffness, [25]. For low velocities in systems with moderate friction, the level at which stick slip will be eliminated corresponds roughly to:

$$\tau_L^* \geq \pi \quad \text{or} \quad k_p \geq M\frac{\pi^2}{\tau_L^2}. \tag{30}$$

Illustrated in Fig. 9 is the stick-slip extinction boundary as a function of normalized stiffness, k_p/M, and dimensionless desired velocity, $\dot{\xi}_d$. The extinction boundary is shown for several values of damping, ρ. The figure was obtained by evaluating (28) using the parameters of the PUMA joint 1, exclusive of γ, which is set to zero for Fig. 9. The parameters of the PUMA joint 1 are: $M = 6.3$ [kg-m^2], $F_{s,\infty} = 1.6$ [kg-m/s^2], $\tau_L = 0.050$ [s], $\gamma = 0.264$ [s], $\dot{x}_s = 0.0058$ [rad/s], $F_v = 4.94$ [N-m/rad/s], [2], [5]. The region below a stick-slip extinction boundary comprises combinations of system stiffness and desired velocity for which stick slip will occur, as indicated by (28) and the condition $\Delta_{E^*_{\text{slip}}} \geq -\Delta_{E^*_w}$. In the region above an extinction boundary $\Delta_{E^*_{\text{slip}}} < -\Delta_{E^*_w}$ and stick slip will not occur. As expected, the regime of stick slip is reduced by increasing ρ. More intriguing is the fact that the required damping is a decreasing function of stiffness, and, perhaps unexpectedly, there are values of stiffness and desired velocity for which stick slip will not occur, even if the system possess no damping. Systems which exhibit smooth motion in the absence of damping are possible because of the influence of frictional memory. The unusual mix of physical and dimensionless coordinates in Fig. 9, as well as Fig. 12, 13, and 14, was chosen to enhance interpretation. In the dimensional analysis, stiffness is scaled to unity; and it is friction, $F_{s,b_n}(\gamma^*, t_2^*)$, which scales inversely with physical stiffness and could be used as the dimensionless ordinate variable. But stiffness, rather than friction, is normally a variable under engineering control. When $\tau_L = 0.050$ [s], $k_p/M = 1974.0$ [rad/s^2] corresponds to $\tau_L^* = \pi$; this is approximately the value of normalized stiffness at which the undamped system of Fig. 9 is stabilized for low velocity motions.

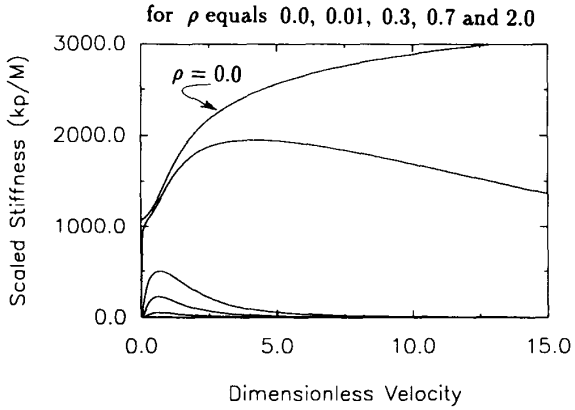

Fig. 9. Stick-slip extinction boundary under the influence of frictional memory. Calculated using equation (28) with $\tau_L = 0.050$ seconds and $F^*_{s,b_n} = F^*_{s,\infty}$ (rising static friction not considered).

IV. The Impact of Rising Static Friction

The level of static friction at breakaway, F_{s,b_n}, is not constant. During motion the level of friction decreases. When motion stops, the static friction builds with time from a reduced value to its ultimate steady state value. This process is illustrated in Fig. 2. The process is one of the lubricant creeping out of the asperity junction sites. The implications of rising static friction for stick slip are substantial: if the length of dwell time, t_2, is short in relation to the static friction rise time, γ, the static friction at breakaway is reduced and the amplitude of the stick-slip cycle diminished. As the amplitude of the stick-slip cycle is diminished, the dwell time is reduced and thus the level of static friction further reduced. If an equilibrium is not reached in this cycle of diminishing static friction and dwell, stick slip will be extinguished. The tribology of this process is discussed in [25], [26] and [20], and an analysis of the impact of rising static friction on stick slip—not considering Stribeck friction or frictional memory—is presented in [13].

The interaction between sliding friction and the rise of static friction is not fully understood. One issue that is uncertain, but must be quantified to support analysis, is the level of friction from which the rise of static friction begins, $F_{s,a}$. Derjaguin *et al.*, [13], employ a static plus Coulomb friction model and presume that the rise of static friction commences from the level of Coulomb friction. Rabinowicz, [26], suggests that at the instant of arriving at zero velocity, indicated by t_a, or $t_2 = 0$, the increase of static friction over sliding friction will be zero. If we consider a more complicated sliding friction model, one governed by the Stribeck curve and delay, a more complicated friction condition exists at t_a: the level of sliding friction rises as the system decelerates. Rising sliding friction is shown by the data of Hess and Soom, [19]. The data from several sources, [28], [34], [6], [21], [19], suggest that the sliding friction rises to the level of static friction, $F_{s,\infty}$ as *steady state* velocity approaches zero. Based on these data, a model to be used for analysis is proposed here.

In Fig. 10 a hypothetical velocity profile and corresponding friction profiles are shown. Curve 10(a) is the velocity profile and curves 10(b) and 10(c) are friction profiles of two possible friction models. Curves 10(b) and 10(c) differ at time t_a. The friction profile of curve 10(b) is that given by the Stribeck friction curve and no frictional

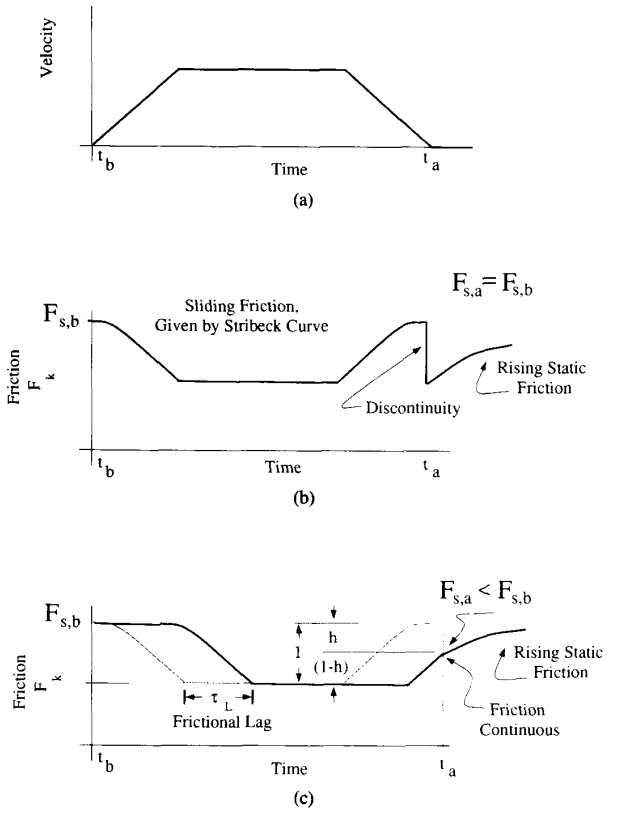

Fig. 10. Two possible starting points for the rise of static friction (a) Velocity profile. (b) Model neglecting frictional lag, friction discontinuous at t_a. (c) Model considering frictional lag, friction continuous at t_a.

memory ($\tau_L = 0$). If the static friction were to start its rise from the level of Coulomb friction, as suggested in [13], a sudden drop in friction at t_a would be required, this is because sliding friction increases from the level of Coulomb friction as velocity diminishes.

An alternative model provides that the rise of static friction begins from the level of sliding friction at t_a, as shown schematically in Fig. 10(c). The level of sliding friction at t_a, F_{s,a_n}, will be less than the value of static friction at breakaway, F_{s,b_n}, because of the interaction of system deceleration, frictional memory and Stribeck friction. Such a friction model is consistent with the dynamic friction model, allows sliding friction to go to the static friction value as steady-state velocity goes to zero, and provides that friction is not discontinuous at the instant t_a. Using this model, the interaction of F_s, γ and τ_L will be studied. This portion of the analysis is not facilitated by the dimensional analysis and will be carried out in physical coordinates.

To represent the degree to which friction is reduced at time t_a the variable h is introduced:

$$F_{s,a_n} = (1 - h)F_{s,b_n}. \tag{31}$$

The variable h ranges from zero to one. Physically, h relates to the lubricant film thickness at the end of the slip. If deceleration is rapid and the film has not had time (relative to τ_L) to become thin, the force required for breakaway—were breakaway to occur at the instant of arrest—would be the level of Coulomb friction: $h = 1$, $F_{s,a_n} = 0$. If deceleration is slower, the lubricant film will have been thinned during the period of low velocity motion and the force required for breakaway would be larger than the level of Coulomb friction: $h = 0$, $F_{s,a_n} = F_{s,b_n}$. In either case, after t_a F_s begins to grow according to (6) and ultimately reaches $F_{s,\infty}$, its highest and steady-state value.

Using the friction model, (6), and the unperturbed trajectory, (23), h can be evaluated:

$$h = \frac{\dot{\xi}_d^2(1 - \cos(\tau_L^*))^2}{\dot{\xi}_d^2(1 - \cos(\tau_L^*))^2 + 1} = \frac{\dot{x}_d^2(1 - \cos(\omega\tau_L))^2}{\dot{x}_d^2(1 - \cos(\omega\tau_L))^2 + \dot{x}_s^2}; \tag{32}$$

$$h \approx \frac{1}{4}\left(\frac{\dot{x}_d}{\dot{x}_s}\right)^2(\omega\tau_L)^4. \tag{33}$$

The approximation, (33), is the first term of the Taylor series expansion and is valid when h is small. When the approximation would give a value of h larger than one, $h = 1$ may be used: h cannot be greater than one. Combining the approximation and upper limit on h yields:

$$h \approx \begin{cases} \frac{1}{4}\left(\frac{\dot{x}_d^2}{\dot{x}_s^2}\right)^2(\omega\tau_L)^4, & k_p\dot{x}_d < \frac{2M\dot{x}_s}{\tau_L^2} \\ 1, & k_p\dot{x}_d \geq \frac{2M\dot{x}_s}{\tau_L^2}. \end{cases} \tag{34}$$

Combining the definition of h, (31), and the rising static friction model, (2), gives a discrete recursive equation for the level of static friction at the moment of breakaway, t_{b_n}:

$$F_{s,b_n} = (1 - h)F_{s,b_{n-1}} + \left(F_{s,\infty} - (1 - h)F_{s,b_{n-1}}\right)\frac{t_2}{t_2 + \gamma}$$

$$= \frac{F_{s,\infty}t_2 + \gamma(1 - h)F_{s,b_{n-1}}}{t_2 + \gamma}. \tag{35}$$

Equation (35) is more complex than it appears, because t_2 depends upon F_{s,b_n}. A larger F_{s,b_n} contributes to a larger $\Delta_{E_w^*}$ and $\Delta_{E_{fs}^*}$; both of which contribute to a larger r_a, resulting in a longer distance to travel during the stick portion of the cycle and thus a longer dwell time. The dependence of t_2 upon F_{s,b_n} is given by:

$$t_{2_n} = \frac{x_{a_{n-1}} - x_{b_n}}{\dot{x}_d} \approx \frac{2F_{s,b_{n-1}}/k_p}{\dot{x}_d}. \tag{36}$$

Substituting the approximation of (36) into (35) gives:

$$F_{s,b_n} = \frac{F_{s,b_{n-1}}\left(F_{s,\infty} + \frac{1}{2}(1-h)k_p\dot{x}_d\gamma\right)}{F_{s,b_{n-1}} + \frac{1}{2}k_p\dot{x}_d\gamma}. \quad (37)$$

To facilitate analysis of the stability of (37), we write:

$$F_{s,b_n} = \frac{F_{s,b_{n-1}}a}{F_{s,b_{n-1}} + b}; \quad (38)$$

where

$$a = \left(F_{s,\infty} + \frac{1}{2}(1-h)k_p\dot{x}_d\gamma\right);$$

$$b = \frac{1}{2}k_p\dot{x}_d\gamma;$$

$$b, F_{s,b} > 0.$$

The parameter b is evidently greater than zero (the sgn$(\cdot)$ functions of (4) handle the case that one might choose $\dot{x}_d < 0$). The existence of a stick-slip cycle is a necessary condition for the validity of update (37), giving rise to the requirement that $F_{s,b} > 0$.

The map $F_{s,b_{n-1}} \rightarrow F_{s,b_n}$ has two fixed points: $F_{s,b_{n-1}} = 0$ and $F_{s,b_{n-1}} = (a-b)$. When $a > b$, the fixed point $F_{s,b_{n-1}} = 0$ is a repulsor, that is it is unstable; and the fixed point $F_{s,b_{n-1}} = (a-b)$ is an attractor, a stable fixed point. The update of (38) is nonlinear, but near the steady state it will converge with rate $((a-b)/a)^n$, where n is the index on stick-slip cycles. Away from the steady state the convergence rate is faster. Expressing the fixed point $F_{s,b_n} = (a-b)$ in the parameters of the friction model yields $F_{s,b_{ss}}$, the steady state value of $F_{s,b}$:

$$F_{s,b_{ss}} = F_{s,\infty} - \frac{1}{2}hk_p\dot{x}_d\gamma. \quad (39)$$

When $(a-b) \leq 0$ there is no fixed point greater than zero. With rate not less than $(a/b)^n$, F_{s,b_n} will decay to zero. As F_{s,b_n} decays to zero, stick slip is extinguished. Expressing the requirement $(a-b) > 0$ in terms of the parameters of the friction model yields the necessary condition for stick slip:

$$F_{s,\infty} > \frac{1}{2}hk_p\dot{x}_d\gamma. \quad (40)$$

When $F_{s,\infty} \leq (1/2)hk\dot{x}_d\gamma$ there can be no stable stick-slip limit cycle. A system operating in this condition may experience several stick-slip cycles, simulation and experiment show this to happen; but the level of static friction decays steadily and ultimately any nonzero damping is sufficient to extinguish the stick-slip cycle. Note that even though (39) can yield a negative value of the steady state F_{s,b_n}, (37) will never actually give a negative value: F_{s,b_n} decays until stick slip is extinguished.

Fig. 11 is a plot of the steady-state breakaway friction as a function of sliding velocity and stiffness, given by equation (39). The stick-slip cycle amplitude is related directly to the magnitude of breakaway friction. The figure shows the model to predict a stick-slip cycle that diminishes abruptly when the critical velocity is reached. This is the process described by Rabinowicz, [25], and illustrated with empirical data in Fig. 4.

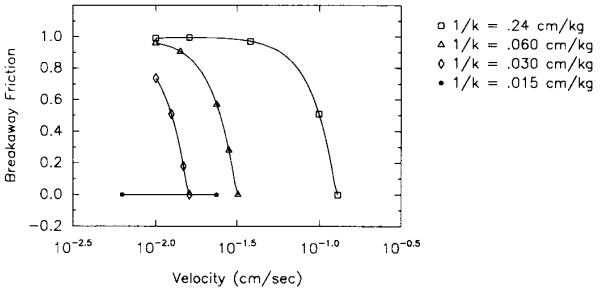

Fig. 11. Stick slip amplitude as a function desired velocity for several values of stiffness.

The parameter h may itself depend upon velocity and stiffness, as shown by (34). Considering this interaction, the stick-slip extinction boundary, the boundary in system parameter space on which $F_{s,b_{ss}} = 0$ is given by:

$$k_p\dot{x}_d \geq \begin{cases} 2\dfrac{F_{s,\infty}}{\gamma}, & \dfrac{F_{s,\infty}}{\gamma} > \dfrac{M\dot{x}_s}{\tau_L^2} \\ 2\sqrt[3]{\dfrac{F_{s,\infty}}{\gamma}\dfrac{M^2\dot{x}_s^2}{\tau_L^4}}, & \dfrac{F_{s,\infty}}{\gamma} \leq \dfrac{M\dot{x}_s}{\tau_L^2} \end{cases} \quad (41)$$

The case statement arises from the cases of (34).

Plotted on the stiffness-velocity plane, (41) produces a curve $k_p \propto (1/\dot{x}_d)$; where the constant of proportionality is given by the dynamic and friction parameters of the system. In Fig. 12 the $\rho = 0$ curve is the contour given by (41), evaluated using the PUMA joint 1 parameters. This line is the extinction boundary due to the rise time of static friction when the system is undamped. As expected, Fig. 12 shows that smooth motion is more easily obtained as desired velocity is increased.

Using (39), the steady-state static-friction level may be determined:

$$F_{s,b_{ss}} = F_{s,\infty} - \frac{1}{2}hk_p\dot{x}_d\gamma;$$

$$F^*_{s,b_{ss}} = \frac{F_{s,b_{ss}}/M}{\omega\dot{x}_s}. \quad (42)$$

Incorporating $F_{s,b_{ss}}$ into (28) yields the complete condition for eliminating stick slip:

$$-2\pi\rho\dot{\xi}_d^2 + F^*_{s,b_{ss}}\dot{\xi}_d\Delta'_{E^*_{Fs}} < -\frac{1}{2}\left(F^*_{s,b_{ss}}\frac{\dot{\xi}_d^2}{1+\dot{\xi}_d^2}\right)^2 \quad (43)$$

Equation (43) reflects the full friction model: nonlinear Stribeck friction, frictional memory and rising static fric-

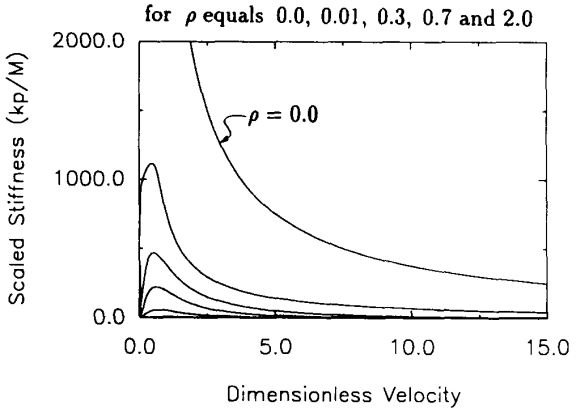

Fig. 12. Stick-slip extinction boundary under the influence of rising static friction, $\gamma = 0.264$ s. The $\rho = 0$ contour was calculated using (41); other contours were calculated using (43). ($\tau_L = 0$, frictional memory not considered.)

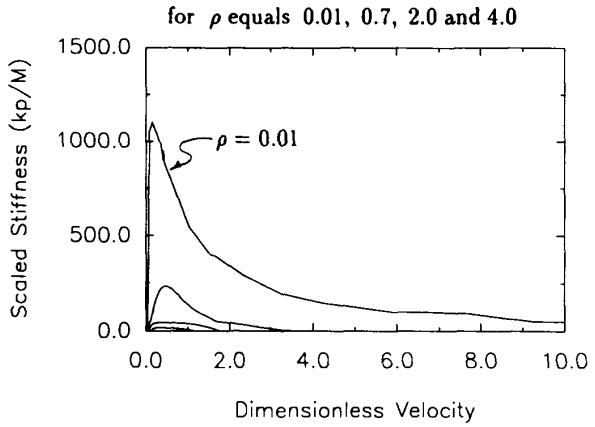

Fig. 13. Stick-slip extinction boundary as a function of stiffness and desired velocity; determined by numerical integration of (4).

tion are considered. The contour on which $\Delta_{E^*_{slip}} < -\Delta_{E^*_w}$ is the stick-slip extinction boundary: those combinations of parameters where dissipation is just sufficient to remove the energy inserted by spring windup. Equation (43) was used to calculate the $\rho = 0.01$, 0.3, 0.7, and 2.0 contours of Fig. 12, and the $k'_v = 4.9$ contour of Fig. 14. Fig. 12 should be contrasted with Fig. 9, where rising static friction is not considered. It is important to model rising static friction to correctly capture the extinction of stick slip with rising velocity.

Equation (43) provides the means to predict the presence of stick slip using system and friction parameters. The analysis is approximate; the perturbation analysis, Taylor series expansion and approximation of t_2, as well as assumptions in the underlying physical modeling of rising static friction, all contribute to the uncertainty of the result. The usefulness of the result for a specific range of parameters can be assessed by comparison with the results of numerical investigation. And, of course, when experiment is available, it can be used to test the validity of the approximate analytic result.

Fig. 13 was generated by numerical integration of (4). The stabilizing value of ρ was determined by iteration at each of 8,000 points. The iso-ρ contours were created by interpolation. Damping levels calculated with (43), presented in Fig. 12, are conservative, but otherwise reflect the simulation values quite well.

Verifying theory by experiment, the results of 17 experimental trials are shown in Fig. 14, along with the extinction boundary calculated using equation (43) and the measured frictional damping of $F_v = 4.9$ [N-m/rad/s]. Of the 17 experimental trials in Fig. 14, 6 show smooth motion. All of these lie above the stick-slip extinction boundary. Of the 11 trials that show stick slip (two trials lie near to each other at $\dot{\xi}_d = 0.85$, $k_p/M = 320$), 10 would be predicted to stick-slip by this analysis. The 11th appears to be an outlier. The evaluation of the theoretical model is based upon the directly measured friction parameters presented in [2], [5]; there is no parametric fitting of the friction model to the locations of the experimental points shown in Fig. 14.

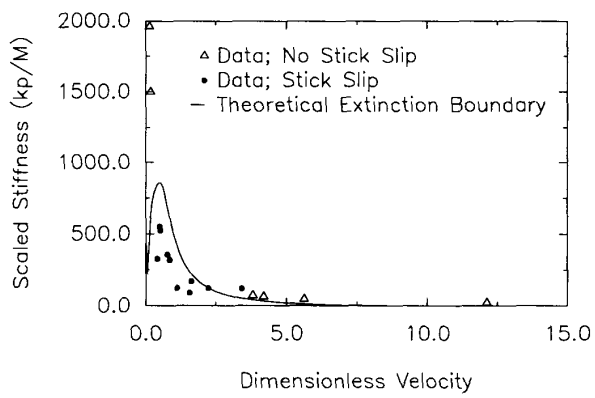

Fig. 14. Experimental stick-slip data; the solid contour is the stick-slip extinction boundary calculated with the condition $\Delta_{E^*_{slip}} < -\Delta_{E^*_w}$.

V. Conclusion

Dimensional and perturbation analysis have been applied to the problem of nonlinear low-velocity friction. Through dimensional analysis an exact model of the nonlinear system can be formed in five parameters rather than ten, greatly facilitating study and explicitly revealing the interaction of parameters. By converting the system of differential equations into a set of integrations, the perturbation technique makes approximate analysis possible where only numerical techniques had been available before. Comparison of Figs. 9 and 12 with Fig. 13 shows the approximation to be valid over a broad range of system parameters and operating conditions. Calculated using the measured friction parameters of the PUMA arm, the predicted regions of stick slip shown in Fig. 14 agree remarkably well with experimental observation.

In contrast with analyses based on the.Coulomb + viscous + static friction model, the present analysis—based on a model with Stribeck friction, rising static friction and frictional memory—is able to account for observed phenomena of mechanisms: that a mechanism with PD control may exhibit stick slip, that stiffening a mechanism may eliminate stick slip, and that certain lubricants—those with a long rising static friction constant—are particularly effective in eliminating stick slip. Furthermore, the agreement of model-based prediction and experimental observation of stick slip is unique and provides a new basis for engineering precision servos.

The work presented provides an analysis tool for predicting stick slip in a proposed control system design. It specifically considers steady, low-speed motions where stick slip is often a challenge. A control design methodology is not directly implied by this analysis tool. But coupled with standard design methodologies and engineering knowledge of the system at hand, the ability to predict the operating conditions for stick slip will provide the ability to choose design parameters without lengthy hand tuning procedures. Additionally, the closed-loop control implications of mechanical parameters, such-as transmission stiffness and lubrication, can be evaluated.

The dimensional and perturbation analysis techniques also provide a basis for the study of more specialized control schemes. Variable structure control (VSS, for Variable Structure System) is, for example, strongly indicated by the need near zero velocity for control stiffness that may be impractical at larger velocities. Various VSS schemes may be studied within the dimensional and perturbation analysis framework by ensuring that the unperturbed trajectory provides a good approximation of the true trajectory and performing the appropriate integrations.

Extending this analysis to cases of velocity reversal and systems with integral control are topics of continuing research. Correct consideration the energy transactions arising during a velocity reversal will require incorporating presliding displacement into the friction model. In tribology and in controls, work proceeds toward a better understanding of the phenomena of low speed motion. As this understanding improves, dimensional and perturbation analysis will continue to provide a handle on system behaviors that do not yield to exact analysis.

REFERENCES

[1] B. Armstrong-Hélouvry, P. Dupont, and C. Canudas de Wit, "A survey of models, analysis tools and compensation methods for the control of machines with friction," *Automatica*, 1994, in Press.

[2] B. Armstrong-Hélouvry, *Control of Machines with Friction*. Boston: Kluwer Academic Press, 1991.

[3] ——, (May), "Strick-slip arising from stribeck friction," in *Proc. 1990 Inter. Conf. Robotics Automation*, Cincinnati, OH, 1990, pp. 1377–82.

[4] B. Armstrong, "Control of machines with nonlinear low-velocity friction: A dimensional analysis," in *Proc. First Int. Symp. Experimental Robotics*, Montreal, Quebec, June, 1989, pp. 180–95.

[5] ——, 1988, "Dynamics for robot control: Friction modeling and ensuring excitation during parameter identification," Ph.D. dissertation, of Electrical Engineering, Stanford Univ., May 1988; Stanford Computer Science Memo STAN-CS-88-1205.

[6] R. Bell and M. Burdekin, "Dynamic behavior of plain slideways," in *Proc. Inst. Mech. Eng.*, vol. 181, pt. 1, no. 8, 1966, pp. 169–83.

[7] ——, 1969, "A study of the stick-slip motion of machine tool feed drives," in *Proc. Inst. Mech. Eng.*, vol. 184, pt. 1, no. 29, pp. 543–60.

[8] E. Buckingham, 1914, "On physically similar systems: Illustrations of the use of dimensional equations," *Phys. Rev.*, vol. 4, pp. 345–376.

[9] C. Canudas de Wit, P. Noel, A. Aubin, B. Brogliato, and P. Drevet, "Adaptive friction compensation in robot manipulators: Low-velocities," *Int. J. Robotics Res.*, June 1991.

[10] C. Canudas de Wit and V. Seront, (May), "Robust adaptive friction compensation," in *Proc. Inter. Conf. Robotics Automation*, Cincinnati, May 1990, pp. 1383–1389.

[11] H. Czichos, *Tribology*. Amsterdam: Elsevier, 1978.

[12] P. R. Dalh, "Solid friction damping of mechanical vibrations," *AIAA J.*, vol. 14, pp. 1675–1682.

[13] B. V. Derjaguin, V. E. Push, and D. M. Tolstoi, 1957 (October), "A theory of stick-slip sliding of solids," in *Proc. Conf. Lubrication Wear*, London: Inst. Mech. Engs., pp. 257–68.

[14] P. E. Dupont, "Avoiding stick-slip in position and force control through feedback," in *Proc. 1991 Int. Conf. Robotics Automation*, Sacramento, Apr. 1991, pp. 1470–1476.

[15] ——, "Friction modeling in dynamic robot simulation," in *Proc. 1990 Int. Conf. Robotics Automation*, Cincinnati, May 1990, 1370–1377.

[16] H. E. Ehrich, "An investigation of control strategies for friction compensation," M.S. thesis, Dept. of Mechanical Engineering, University of Maryland, 1991.

[17] A. Gogoussis and M. Donath, "Coulomb friction and drive effects in robot mechanisms," in *Proc. 1987 Int. Conf. Robotics Automation*, Raleigh, Mar. 31–Apr. 3, 1987, pp. 828–36.

[18] D. A. Haessig and B. Friedland, 1991, "On the Modeling and simulation of friction," *J. Dyn. Syst. Measurement Contr.*, vol. 113, no. 9, pp. 354–362, 1991.

[19] D. P. Hess and A. Soom, "Friction at a lubricated line contact operating at oscillating sliding velocities," *J. Tribology*, vol. 112, no. 1, pp. 147–152, 1990.

[20] S. Kato, N. Sato, and T. Matsubay, "Some considerations of characteristics of static friction of machine tool slideway," *J. Lubrication Tech.*, vol. 94, no. 3, pp. 234–247, 1992.

[21] V. E. Khitrik and V. A. Shmakov, "Static and dynamic characteristics of friction pairs," *Soviet J. Friction Wear*, vol. 8, no. 5, pp. 112–115, 1987.

[22] K. C. Ludema, "Engineering progress and cultural problems in tribology," *Lubrication Eng.*, vol. 44, no. 6, pp. 500–509, 1988.

[23] J. A. C. Martins, J. T. Oden, and F. M. F. Simoes, "A study of static and kinetic friction," *Int. J. Eng. Sci.*, vol. 28, no. 1, pp. 29–92, 1990.

[24] A. Polycarpou and A. Soom, "Transitions between sticking and slipping," in *Friction-Induced Vibration, Chatter, Squeal and Chaos*; also in *Proc. ASME Winter Annual Meeting*, Anaheim, CA, DE-vol. 49, R. A. Ibrahim and A. Soom, Eds. New York: ASME, pp. 139–48, 1992.

[25] E. Rabinowicz, *Friction and Wear of Materials*. New York: Wiley, 1965.

[26] ——, "The intrinsic variables affecting the stick-slip process," in *Proc. Physical Society of London*, vol. 71, pp. 668–675, 1958.

[27] J. R. Rice and A. L. Ruina, "Stability of steady frictional slipping," *J. Applied Mech.*, vol. 50, pp. 343–349, 1983.

[28] J. B. Sampson, F. Morgan, D. W. Reed, and M. Muskat, "Friction behavior during slip portion of the stick-slip process," *J. Applied Physics*, vol. 14, no. 12, pp. 689–700, 1943.

[29] C. N. Shen, "Synthesis of high order nonlinear control systems with ramp input," *IRE Trans. Automat. Contr.*, vol. AC-7, no. 2, pp. 22–37, 1962.

[30] R. Stribeck, "Die Wesentlichen Eigenschaften der Gleit- und Rollenlager—The Key Qualities of Sliding and Roller Bearings," *Zeitschrift des Vereines Seutscher Ingenieure*, vol. 46, no. 38, pp. 1342–1348 and vol. 46, no. 39, pp. 1432–1437, 1902.

[31] J. Tou and P. M. Schultheiss, 1953, "Static and sliding friction in feedback systems," *J. Applied Physics*, vol. 24, no. 9, pp. 1210–1217.

[32] W. T. Townsend and J. K. Salisbury, "The effect of Coulomb friction and sticktion on force control," in *Proc. 1987 Int. Conf. Robotics Automation*, Raleigh, 1987, pp. 883–889.

[33] A. Tustin, "The effects of backlash and of speed-dependent friction on the stability of closed-cycle control systems," *IEE J.*, vol. 94, part 2A, pp. 143–151, 1947.

[34] G. V. Vinogradov, I. V. Korepova, and Y. Y. Podolsky, "Steel-to-steel friction over a very wide range of sliding speeds," *Wear*, vol. 10, no. 5, pp. 338–352, 1967.

[35] C. D. Walrath, "Adaptive bearing friction compensation based on recent knowledge of dynamic friction," *Automatica*, vol. 20, no. 6, pp. 717–727, 1984.

[36] A. Xiaolan and Y. Haiqing, "A full numerical solution for general transient elastohydrodynamic line contacts and its application," *Wear*, vol. 121, no. 2, pp. 143–159, 1987.

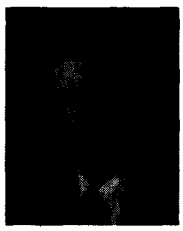

Brian Armstrong-Hélouvry received the B.Sc. degree in physics and mechanical engineering from MIT, Cambridge, MA, in 1980, and the M.Sc. and Ph.D. degrees in electrical engineering from Stanford University, Stanford, CA, in 1984 and 1988.

He joined the Department of Electrical Engineering and Computer Science at the University of Wisconsin, Milwaukee, in 1989. In 1986, 1988, and 1991, he held visiting positions with Mitsubishi Electric Company, Osaka, Japan; INRIA, then in Rennes, France; and the State University of Campinas, Campinas Brazil. His interests include problems of identification and control in robotics and other nonlinear systems.

Dr. Armstrong-Hélouvry has recent published *Control of Machines with Friction*, Kluwer Academic Press.